Calorimetry for LENR

ARPA-E LENR workshop
October 21, 2121

Objectives for calorimeter analysis

- **Prepare any claimed result for rigorous review**
  - An error bar on every data point; quantified uncertainty on every claim
  - Build multiple copies of your experiment. Recalibrate and run replicates as you go.
  - Share and archive all data and metadata for independent review.
  - Calibrate the instrument over wider excursions in time and power than the experiment.
    - Earn your license to go excess heat hunting. This can take a year or more of preparation.
  - Deploy primary and backup sensors.
  - Model and explain all of the sensor data.
  - Include control experiments that rule out prosaic hypotheses
  - Document the methods and the thread of reasoning from raw data to conclusion

Objectives for calorimeter analysis continued

- **During calibration, discover in the data what a human might miss**
  - Avoid the human foible of observer bias
    - What are all of the possible ways this could not be excess heat?
  - Learn the system behavior very well so that during experiments deviations from model predictions can be trusted as significant
- **During experimentation**
  - Continue calibration and control runs throughout to control for apparatus drift
  - If something looks interesting, seek independent laboratory replication

An error bar on every data point

Example: high pressure high temperature metal hydride

- each experiment in quadruplicate
- vertical lines 95% confidence about average
- 3 sigma detection limit shown

https://doi.org/10.1038/s41586-019-1256-6

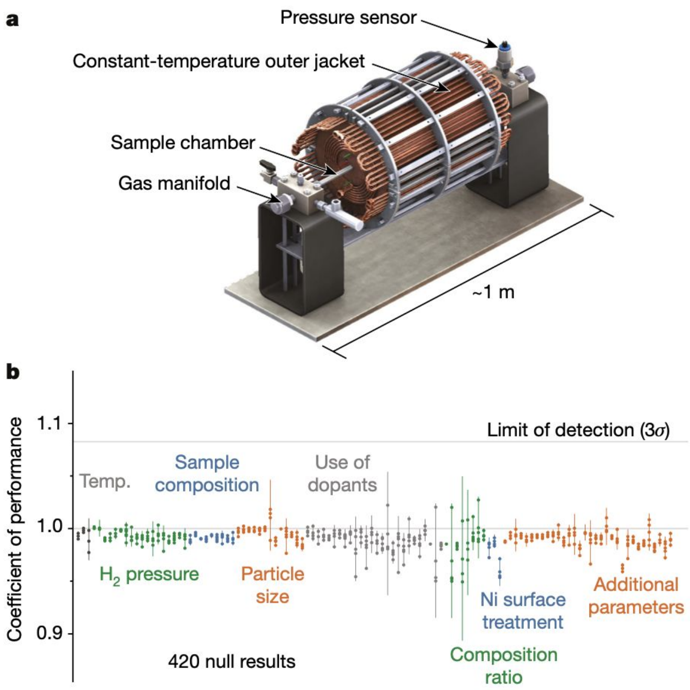

Fig. 3 | Detecting excess heat at high temperatures. a, Rendering of a calorimeter capable of testing for excess heat production at high temperatures and high hydrogen pressures. The calorimeter features a cylindrical alumina sample chamber and 14 independent thermocouple sensors (not visible) within a constant-temperature outer jacket. The ends of the sample chamber are connected to gas manifolds, one of which is equipped with a pressure sensor. **b**, Plot of coefficient of performance (COP) as a function of the independent variable (shown in coloured text) to evaluate claims of excess heat production by the Ni–H materials system. Each unique experimental condition was typically sampled in quadruplicate. The 3σ limit of detection is presented as a solid grey horizontal line at COP = 1.0825. Dots, 420 individual sample runs; vertical lines, 95% confidence intervals about the average.

An error bar on every data point

Example: Letts experiment replication

- Faithful reconstruction of apparatus
- Calibration revealed apparatus failures capable of producing >100 mW artifacts.
- After fixing failure modes, no excess heat observed.

Attempted Replication of Excess Heat in the Letts Dual-laser Experiment
Mason J. Guffey, Yang Tang and P.J. King : ReResearch LLC, 3519 Jack Northrop Ave., Hawthorne, CA 90250, USA

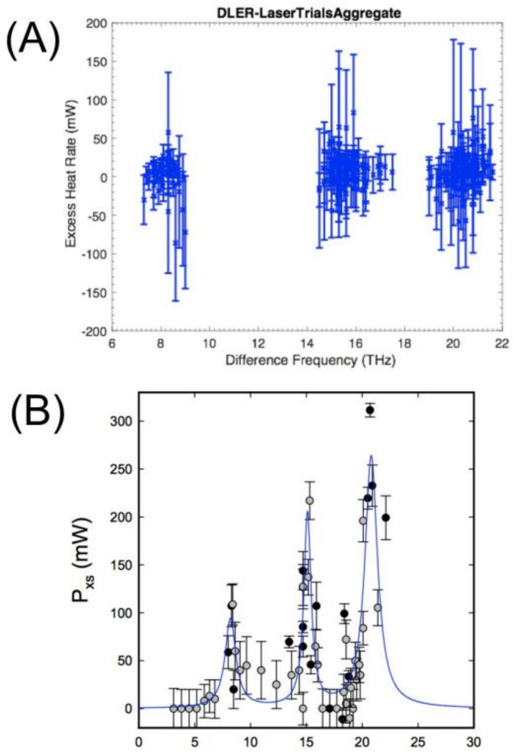

Figure 9. (A) Aggregated calorimetric data obtained for all laser trials discussed in this study. Error bars are 1 sigma standard deviations. (B) Excess heat as a function of detuning taken from reference 7.

Report all your data

Example: high pressure high temperature metal hydride

- 420 null results

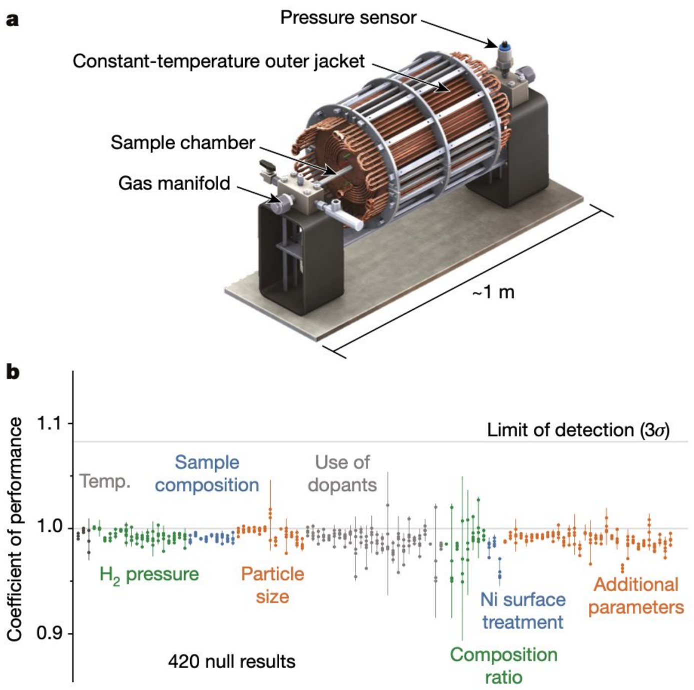

Fig. 3 | Detecting excess heat at high temperatures. a, Rendering of a calorimeter capable of testing for excess heat production at high temperatures and high hydrogen pressures. The calorimeter features a cylindrical alumina sample chamber and 14 independent thermocouple sensors (not visible) within a constant-temperature outer jacket. The ends of the sample chamber are connected to gas manifolds, one of which is equipped with a pressure sensor. **b**, Plot of coefficient of performance (COP) as a function of the independent variable (shown in coloured text) to evaluate claims of excess heat production by the Ni–H materials system. Each unique experimental condition was typically sampled in quadruplicate. The 3σ limit of detection is presented as a solid grey horizontal line at COP = 1.0825. Dots, 420 individual sample runs; vertical lines, 95% confidence intervals about the average.

https://doi.org/10.1038/s41586-019-1256-6

Archive all the data

One second of data

DateStamp	**13/04/2017**
TimeStamp	**11:43:13.134**
Pressure_1	0.955631348
Voltage_1 (V)	6.944
Current_1 (A)	20.114
Resistance_1 (Ω)	0.345230402
Voltage_2 (V)	6.923175271
Power_1 (W)	139.2606601
Internal Top	180.8140906
Internal Bot	158.843144
Back Brick Top Mid	89.43193378
Back Brick Bot Mid	70.63432485
Back Brick Top L	72.11884765
Back Brick Bot R	51.50715517
Front Brick Top Mid	64.35528123
Front Brick Bot Mid	67.73211302
Surface Can Top L	16.73702861
Surface Can Top R	16.66714854
Surface Can Bot R	16.49421933
Surface Can Bot L	16.56916057
Back Face Plate	17.91205576
Front Face Plate	19.18418332

× 7 instruments

One experiment

4 instruments × 2 days ≈ 13,800,000 data points

All experiments

100 HTC experiments ≈ 1.38 billion data points

Archive all the data

Reanalysis may prove very important later on

1998 EPRI Report TR-107843-V1

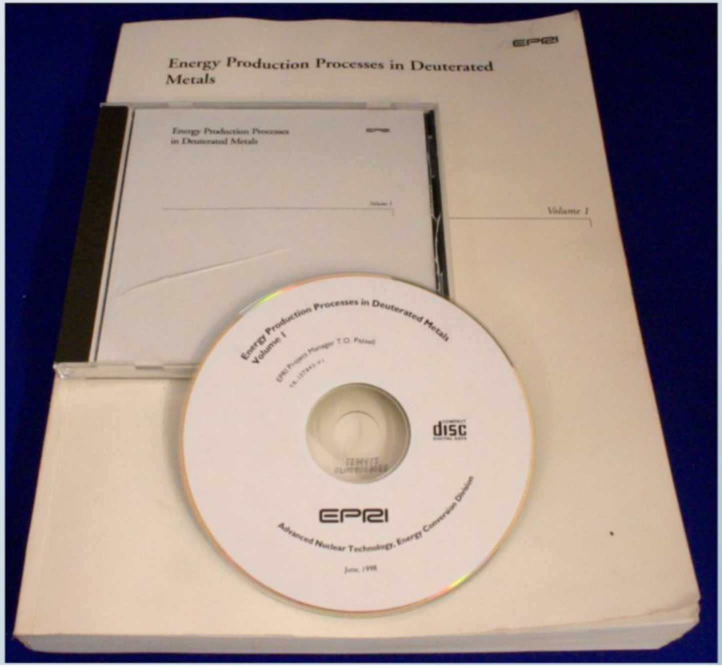

Calibrate outside the experimental operating conditions

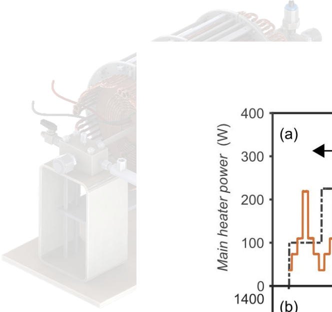

Rev. Sci. Instrum. **88**, 084101 (2017)

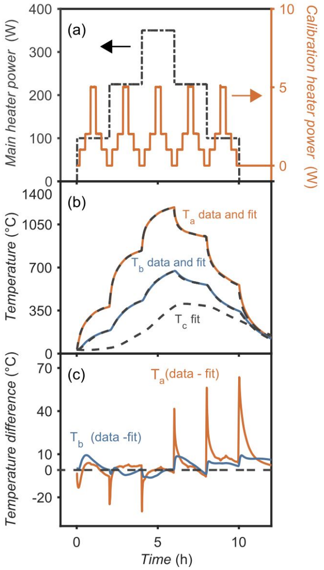

FIG. 6. Calibration experiment input powers, measured system temperature response, model fits, and fit residuals. (a) Time-varying input powers to the main heater and calibration heater, both of which are 0 W at *time* = 0. (b) Temperature response of the instrument to the inputs as measured experimentally and as simulated with the model using the optimized parameter values. Only simulated data are shown for T_c as this is an unmeasured node. The fits of the simulated temperatures to the measured data are shown in dashed lines (c) Temperature residuals (data less fit) for the T_a and T_b nodes. The poor fit at the T_a node near the large step changes in the main heater power indicates that the high-frequency dynamics of the T_a node are not very well described by the present model and that additional model refinement in that region would be beneficial.

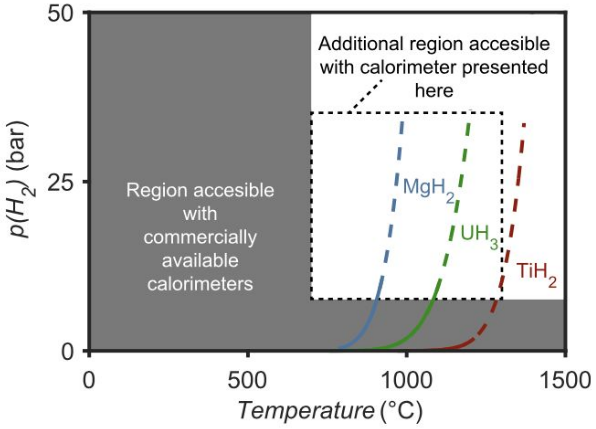

FIG. 1. Range of operation for commercially available calorimeters (grey shaded region; see Table SI of the supplementary material for details) and for the instrument reported here that enables calorimetric studies in a previously inaccessible temperature and hydrogen pressure regime. Decomposition pressure-temperature curves for selected metal hydride systems are indicated; the solid parts of the curves are data extracted from Sandrock's review of hydrogen storage materials,[4] and the dashed parts of the curves are extrapolations from that data according to the van't Hoff equation.

Rev. Sci. Instrum. **88**, 084101 (2017)

Google

Deploy primary and backup sensors

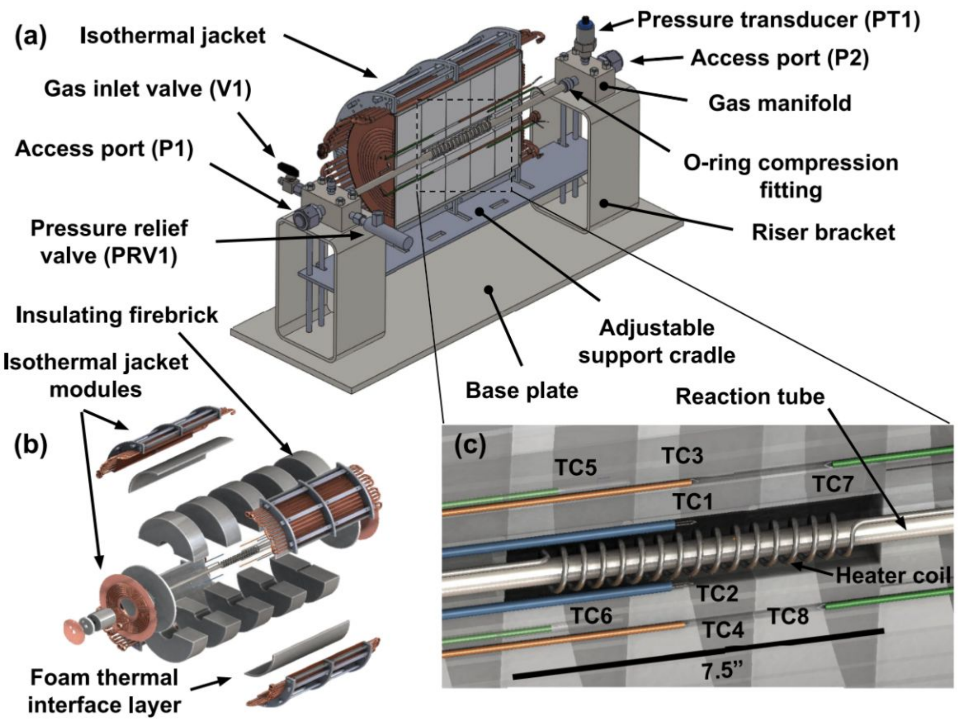

FIG. 2. Mechanical design of the calorimeter. (a) Overview of the instrument with one half of the isothermal jacket and furnace insulation cut away. (b) Exploded view of the furnace, showing the ten insulating fire bricks and the surrounding modular isothermal jacket consisting of four quadrants, two end plates, and corresponding elastic foam thermal interface layers. (c) Detailed view of the hot zone showing the locations of the heater and the eight internal thermocouples (orange, green, and blue cylinders, TC1–TC8). Not shown are six additional thermocouples epoxied to the isothermal jacket (TC9–TC14), one on each quadrant and each end plate.

Rev. Sci. Instrum. **88**, 084101 (2017)

Model and explain all of the sensor data

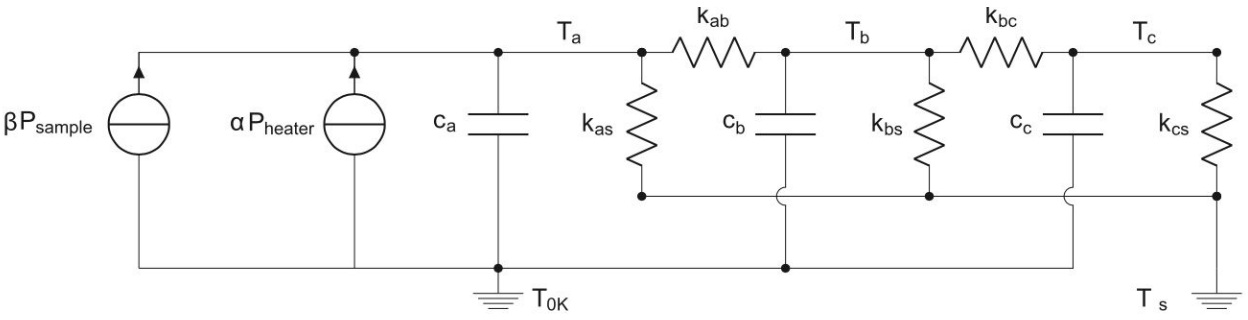

FIG. 5. The two-source, three-state, lumped-element heat flow model of the instrument used to infer the sample power from temperature data. The power from the sample or from a calibration heater at the sample position, P_{sample}, and the power from the main heater P_{heater} are modeled as current sources with temperature-dependent scale factors α and β, which account for the temperature dependence of the radiative and conductive coupling of the heat sources to the sensors. Heat capacities at the nodes i are modeled as capacitors c_i and conductances between nodes i and j are modeled as conductances k_{ij}.

Rev. Sci. Instrum. **88**, 084101 (2017)

Model and explain all of the sensor data

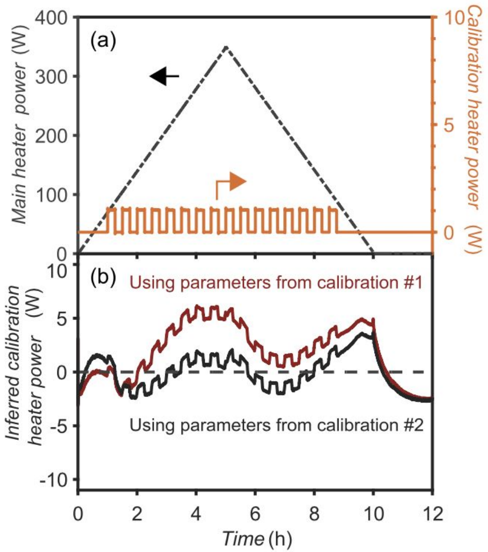

FIG. 7. Summary of calorimetric data from the exotherm simulation experiment. (a) The input powers to the main and calibration heaters. (b) The calibration heater power as inferred using the two different calibrations. The difference between the two inferred power curves suggests that some run-to-run fluctuations are occurring in the instrument. The input power pulses are clearly recovered despite a baseline of several watts. We attributed this baseline to imperfect modeling of the heat flows by the lumped-element model. A model artifact due to the rapid change in the sign of the main heater input power ramp rate is clearly visible in the inferred sample power at 5 h.

$$\frac{dT_a}{dt} = \frac{1}{c_a}\left(\beta P_{sample} + \alpha P_{heater} - k_{as}(T_a - T_s) - K_{ab}(T_a - T_b)\right), \tag{1a}$$

$$\frac{dT_b}{dt} = \frac{1}{c_b}\left(k_{ab}(T_a - T_b) - k_{bs}(T_b - T_s) - k_{bc}(T_b - T_c)\right), \tag{1b}$$

$$\frac{dT_c}{dt} = \frac{1}{c_c}\left(k_{bc}(T_b - T_c) - k_{cs}(T_c - T_s)\right), \tag{1c}$$

where

$$c_i = c_{i,0} + c_{i,1}T_i + c_{i,2}T_i^2, \qquad i \in \{a, b, c\}, \tag{1d}$$

$$k_{ij} = k_{ij,0} + k_{ij,1}T_i + k_{ij,2}T_i^2, \qquad ij \in \{as, ab, bs, bc, cs\}, \tag{1e}$$

$$\alpha = \alpha_0 + \alpha_1 T_a + \alpha_2 T_a^2, \tag{1f}$$

$$\beta = \beta_0 + \beta_1 T_a + \beta_2 T_a^2. \tag{1g}$$

Rev. Sci. Instrum. **88**, 084101 (2017)

Energy COP defined

$$COP_{energy}(t) = \frac{\int_0^t \left[P_{out}(t) + P_{stored}(t)\right] dt}{\int_0^t P_{in}(t) dt}$$

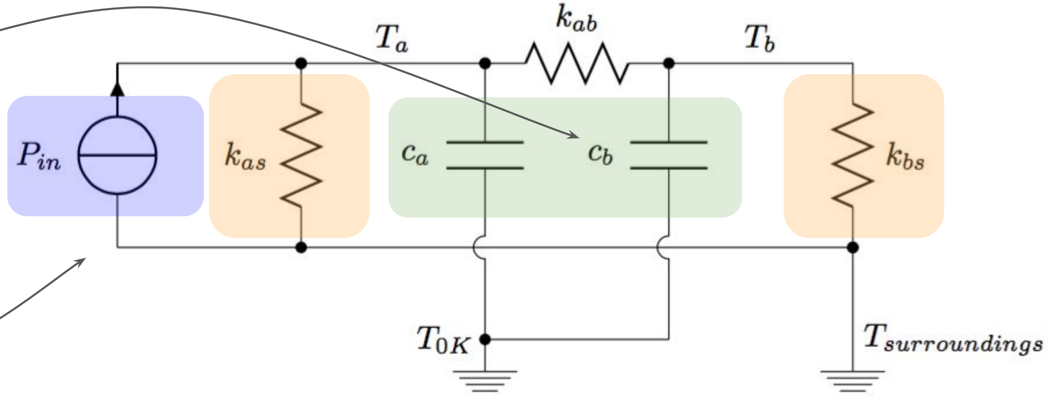

Example equations for a two state two capacitor model

$$P_{out}(t) = k_{as}\left[T_a(t) - T_s(t)\right] + k_{bs}\left[T_b(t) - T_s(t)\right]$$

$$P_{stored}(t) = c_a \frac{dT_a(t)}{dt} + c_b \frac{dT_b(t)}{dt}$$

- c's and k's are determined by calibratior
- P_{in} is measured directly and used as an input to solve the model system

Calculation of energy COP

$$COP_{energy}(t) = \frac{\int_0^t \left[P_{out}(t) + P_{stored}(t)\right] dt}{\int_0^t P_{in}(t)dt}$$

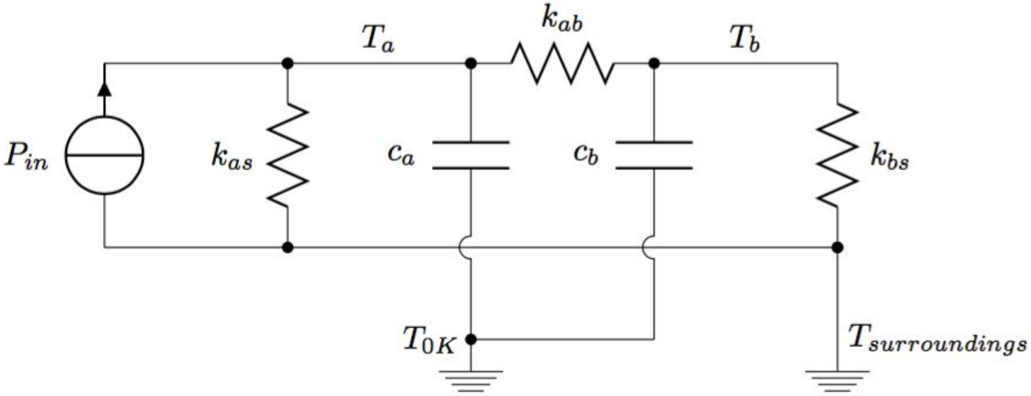

Measured

Calibrated

Calculated

Measured
and
Modelled

$$P_{out}(t) = k_{as}\left[T_a(t) - T_s(t)\right] + k_{bs}\left[T_b(t) - T_s(t)\right]$$

$$P_{stored}(t) = c_a \frac{dT_a(t)}{dt} + c_b \frac{dT_b(t)}{dt}$$

The measured and modeled temperatures give us what we saw and what we expected to see

Google

What about very long measurements?

Include control experiments: From 1998 EPRI/SRI Report

Table 3-1
Overview of Experiments M1-M4

Expt #	Cathode (source) (dimension)	Date (start) (stop)	Duration (hours) (days)	Maximum (D/Pd)	Excess Power (mW)	Excess Power (kJ)
M1	JM* (0.2x3 cm)	3/4/94 5/3/94	1340 (56)	0.927 ± 0.001	180 ± 20	50 ± 25
M2	E#1 (0.3x3 cm)	5/6/94 6/21/94	1104 (46)	0.868 ± 0.001	0 ± 50	0 ± ?
M3	E#4 (0.3x3 cm)	6/24/94 7/5/94	269 (11)	?	0 ± 50	0 ± ?
M4	JM* (0.1x10cm)	7/19/94 9/26/94	1840 (77)	0.944 ± 0.001	400 ± 25	85 ± 25

400 mW ~ 2% of input (21 Watts)

More on calorimetry

Journal of Thermal Analysis and Calorimetry (2019) 138:3139–3157
https://doi.org/10.1007/s10973-019-08271-z

Check for updates

Calorimetry under non-ideal conditions using system identification

B. P. MacLeod[1,4] · D. K. Fork[2] · B. Lam[1] · C. P. Berlinguette[1,3,4]

Received: 13 March 2018 / Accepted: 25 April 2019 / Published online: 15 May 2019

Summary

- Design for reliable operation and low parameter models
- Seek independent review before building
- Design an experiment with far more calibration and control runs than experiment runs
- Seek independent review of your experimental design
- Calibrate both to find failure modes and to establish resolution
- Seek ongoing independent review of your calibration
- Curate and share all the data for independent analysis